J. of Fire Prot. Engr., 7 (1), 1995, pp 1–13

APPLICATIONS OF A MODEL TO PREDICT FLAME SPREAD OVER INTERIOR FINISH MATERIALS IN A COMPARTMENT

J. G. Quintiere, G. Haynes, B. T. Rhodes*
Department of Fire Protection Engineering
University of Maryland
College Park, MD

SUMMARY

Results from a mathematical model are investigated for fire growth on wall and ceiling combustible interior finish material in a compartment. A corner fire ignition source is maintained for 10 minutes at 100 kW and subsequently increased to 300 kW. For this scenario, experimental results are available from the EUREFIC program, and are compared to the model. The time for the total rate of energy release rate to reach 1 MW is examined. In addition to the 11 EUREFIC materials, eight other materials are examined in this scenario by using the model. These materials represent the type of materials formerly and currently used as cabin interior finish materials in commercial aircraft. The model yields good results in most cases; in other cases, the model can be made to yield better agreement with the experimental results by making small changes in the property data. These changes are within the range of uncertainty of the property data.

INTRODUCTION

The purpose of this study is to investigate the accuracy of a mathematical model to predict the fire growth on combustible wall and ceiling interior finish materials in a compartment. The fire scenario is the room corner test as described in the Nordic standard NT Fire 025, or ISO DP 9705. This is similar to the *Proposed Method for Room Fire Test of Wall and Ceiling Materials and Assemblies* considered by ASTM. In the Nordic standard a square propane burner supplies fuel at the base of the corner with an energy release rate of 100 kW for 10 minutes. At 10 minutes, if the total energy release rate from the room does not exceed 1 MW, the burner fire is increased to 300 kW. Although other data are recorded, the principal criterion for the evaluation of the interior finish material is if or when the room energy release rate achieves 1 MW.

The mathematical model has been previously described[1], and compared to room corner test results for 13 materials tested in Sweden[2]. It was found in most cases that the model was reasonably accurate in predicting the outcome of the test to reach 1 MW. Other models have also been successful at predicting these test results. Wickström and Goransson[3] have developed an empirical model, and Karlsson[4] has developed a model similar to the model employed herein. The forerunner to the present model was also used successfully by Cleary and Quintiere[5].

All of these models require material data from the Cone Calorimeter (ASTM E-1354-90, *Standard Test Method for Heat and Visible Smoke Release Rates for Materials and Products Using an Oxygen Consumption Calorimeter*). Wickström and Goransson[3] use data evaluated at an irradiance of 25 kW/m^2, while Karlsson[4] uses data at 50 kW/m^2. The model by Cleary and Quintiere[5] obtained equally good results with cone data selected at both 25 and 50 kW/m^2. The current model attempts to be less arbitrary. It uses derived material property data from the cone calorimeter to calculate the needed information at the heat

*Present address is Hughes Associates, Inc., Baltimore, MD USA.

flux experienced by the material in the room-corner test. Also, the current model and Karlsson's model require data from the LIFT apparatus (ASTM E 1321-90, *Standard Method for Determining Material Ignition and Flame Spread Properties*).

In the current study, the model will be compared to results from a cooperative program in the Nordic countries known as EUREFIC. In this program, 11 widely different materials were tested in the room-corner test, and material data were derived from the cone calorimeter and the LIFT apparatuses.

In addition, the model was run for eight materials representative of past and current commercial aircraft cabin interior linings. Although full-scale post-crash cabin fire experiments exist for some of these materials, no room-corner tests are available. Hence, these results will only show the hypothetical performance of the aircraft materials relative to the Nordic studies.

Summary of Model

The model has been previously described by Quintiere[1], and therefore will only be summarized here. Background for its development, and supportive references will not be repeated here. The model simulates the ignition by the burner, flame spread, burn-out, and burning rate of wall and ceiling materials.

The flame pyrolysis and burn-out fronts are computed with respect to two modes of flame spread. One mode includes upward spread, spread along the ceiling, and spread along the wall-ceiling jet region. This is shown in Figure 1 where the dashed lines enclose the region of wind-aided flame spread due to the burner, and the ceiling jet.

At this time, no distinction for wall and ceiling wind-aided flame spread is made in the model, and they are universally treated as governed by upward flame spread.

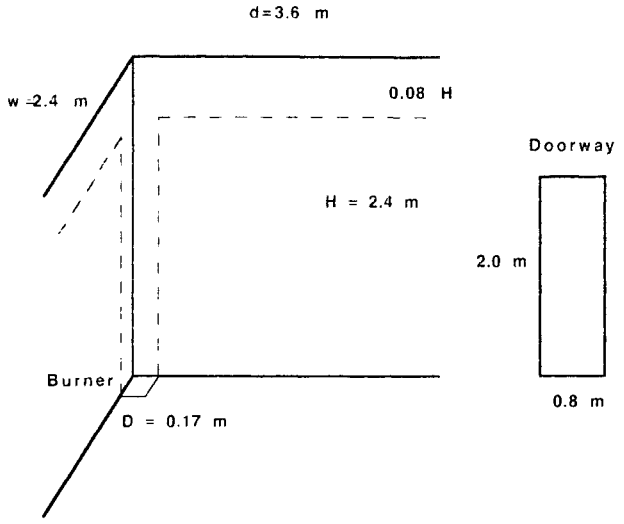

Figure 1. Room and Burner Configuration.

The second mode of spread is composed of lateral spread along the wall and subsequent downward spread from the ceiling jet. Again, the same relationship will be considered for both. In this fashion, the pyrolysis and burn-out areas are computed. An illustration of the pyrolysis (y_p, x_p, and z_p) and burn-out (y_b and x_b) fronts is shown in Figure 2.

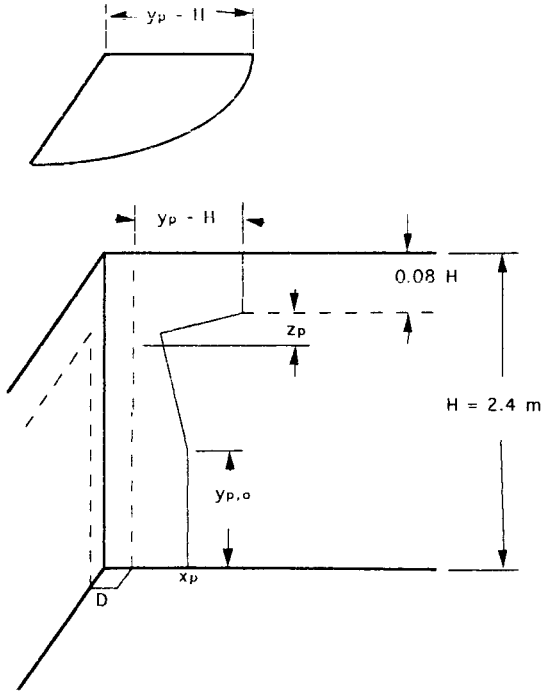

Figure 2. Illustration of Pyrolysis and Burn-out Fronts.

The energy release rate per unit area is computed from the net heat flux in the pyrolysis region. It is considered constant over the pyrolysis area which is computed from the front configuration as a function of time. The energy release rate per unit area is governed by both the flame heat flux and the radiative feedback from the heated room.

Flame heat flux is considered constant over the pyrolysis area, and constant over the extended flame length. Two values are selected: 60 kW/m^2 over the pyrolysis area and for the square burner corner ignition flame which governs burning rate and ignition, respectively; and 30 kW/m^2 for the extended flame region beyond the pyrolysis region which governs upward flame spread.

The room thermal feedback controls both the rate of spread through a computation of the material surface temperature ahead of the flame, and the rate of energy release per unit area through radiative heat transfer from the gas layer in the room. Global models are considered for average room surface and gas layer temperatures. The radiative effects are considered to be maximized to give an upper limit for its effect. This is done by assuming surface and gas layer emissivities of one, and a radiation configuration factor of one between the layer and the room surfaces.

The details for each component of the analysis is summarized below. The symbols are completely defined in the NOMENCLATURE.

Ignition by the Burner Flame

The time for ignition is computed when the propane burner flame heats the wall material to its ignition temperature, *i.e.*, when $T_{s,o} = T_{ig}$. The surface temperature is given by

$$T_{s,o} - T_\infty = \frac{1}{\sqrt{\pi k\rho c}} \int_0^t \frac{q(\tau)}{\sqrt{t-\tau}} d\tau \qquad (1)$$

where $q(\tau) = \dot{q}''_{ig} + \sigma(T^4 - T_{s,o}^4)$,

$\dot{q}''_{ig}$ is the ignitor flame heat flux assumed at 60 kW/m^2, and T is the temperature of the upper gas layer in the room.

The room radiation effect is seen to be maximized in this equation.

Average Upper Gas Layer Temperature, T

$$T = T_\infty \left\{ 1 + C \left[\frac{\dot{Q}}{\rho_\infty c_p \sqrt{g} T_\infty A_o \sqrt{H_o}} \right]^{2/3} \left[\frac{\sqrt{k\rho c / t}\, A_s}{\rho_\infty c_p \sqrt{g} A_o \sqrt{H_o}} \right]^{-1/3} \right\} \qquad (2)$$

where $\dot{Q}$ is the total energy release rate,
A_s is the room surface area,
A_o is the area of the opening,
H_o is the height of the opening,
$k\rho c$ is the thermal inertia of the room lining materials,
$\rho c_p \sqrt{g}$ is 3.44 kW/m$^{5/2}$-K,
and C is the coefficient taken as 2.2 for these corner fires (compared to 1.63 for room-centered fires).

This equation assumes a quasi-steady process.

Room Energy Release Rate, $\dot{Q}(t)$

$$\dot{Q}(t) = \dot{Q}_{ig} + \dot{Q}'' A_p(t) \qquad (3)$$

where $\dot{Q}_{ig}$ is the ignition burner energy release rate,

$\dot{Q}''(t)$ is the energy release per unit area of the material,

and A_p is the pyrolysis area.

Material Energy Release Rate per Unit Area, $\dot{Q}''$

$$\dot{Q}'' = \frac{\Delta H}{L}(\dot{q}_f'' - \sigma T_{ig}^4 + \sigma T^4) \qquad (4)$$

where $\dot{q}_f''$ is the incident flame heat flux over the pyrolysis region (60 kW/m^2),

σT_{ig}^4 is the re-radiation flux loss,

and σT^4 is the incident heat flux from the room.

Pyrolysis Area, A_p

The pyrolysis area is computed from the configuration of the pyrolysis and burn-out fronts as illustrated in Figure 2. Specific formulas for all possible cases are given by Quintiere[1], which are symbolically represented here as

$$A_p = A_p(y_p, y_b, x_p, x_b, z_p, z_b). \qquad (5)$$

The initial area ignited is defined by the burner dimension along the intersecting walls (0.17 m), and by the height of the 100 kW fire which is taken as 1.3 m.

Upward Spread Pyrolysis Front, y_p

The upward fronts are measured from the floor and are taken as continuous distances up the wall and along the ceiling and ceiling jet regions. The upward pyrolysis front is computed from the following differential equation involving the flame length, y_f, and an ignition time based on the average room surface temperature and the flame heat flux:

$$\frac{dy_p}{dt} = \frac{y_f - y_p}{t_{ig}} \qquad (6)$$

where

$$t_{ig} = \frac{\pi}{4} k\rho c \left[\frac{T_{ig} - T_s}{\dot{q}_f''}\right]^2$$

and

$$y_f = y_b + \begin{cases} k_f [\dot{Q}'_{ig} + \dot{Q}''(y_p - y_b)]^n, & y_b < k_f \dot{Q}'^n_{ig} \\ k_f [\dot{Q}'(y_p - y_b)]^n, & y_b \geq k_f \dot{Q}'^n_{ig} \end{cases} \qquad (7)$$

where k_f = 0.01 m^2/kW and n =1.

T_s is computed by Eq.(1) with $q(t) = \sigma(T^4 - T_s^4) + h_c(T - T_s)$, (8)

and h_c = 0.01 kW/m^{2}K as the convective heat transfer coefficient.

$\dot{q}_f''$ is taken as 30 kW/m^2 in the simulation.

$\dot{Q}'_{ig}$ is the energy release rate for the burner which is equivalent to a line-source. It is determined, based on flame length, such that the burner flame length corresponding to $\dot{Q}_{ig}$ is equal to $k_f \dot{Q}_{ig}^n$. It is this flame extension due to the burner fire that can cause the pyrolysis front to propagate in spite of insufficient energy release rate by the material alone. However, when the pyrolysis front extends beyond the burner flame length, it then no longer has any influence on the spread. Hence, it is critical to specify the correct burner flame length. For the 300 kW burner fire, 3.6 m is taken in the model; however, a correlation suggested by Karlsson[4] yields 4.4 m.

Upward Burn-out Front, y_b

$$\frac{dy_b}{dt} \approx \frac{y_p(t) - y_b(t)}{t_b} \qquad (9)$$

gives the differential equation for the burn-out front where

$$t_b = Q''/\dot{Q}''$$

and Q" is the total available energy per unit area which is assumed constant for a given material of a given thickness.

Lateral or Downward Pyrolysis Fronts, x_p or z_p

$$\frac{dx_p}{dt} = \frac{\Phi}{k\rho c\left(T_{ig} - T_s\right)^2} \text{ for } T_s \geq T_{s,min} \qquad (10)$$

where Φ and $T_{s,min}$ are material dependent properties derived from the test procedure of ASTM E-1321. The downward pyrolysis position is given for $t > t_H$, the time when $y_p = H$, as

$$z_p = x_p(t) - x_p(t_H). \qquad (11)$$

Lateral or Downward Burn-out Fronts, x_b or z_b

$$\frac{dx_b}{dt} = \frac{x_p - x_b}{t_b}. \qquad (12)$$

And the downward burn-out front is given by

$$z_b = x_b(t) - x_b(t_H'), \qquad (13)$$

where t_H' is the time when $y_b = H$.

Numerical Solution

Ignition time is determined from the solution of Equation 1, an integral equation for the T_s. A trapezoidal rule, and a Gauss-Siedel iterative process are employed. In addition, a regula falsi iterative method is used to solve Equation 2, an algebraic equation, to obtain T.

Once ignition occurs the differential equations for the fronts are integrated by a second order Runga-Kutta method, and the entire set are simultaneously solved advancing in time.

Materials and Their Properties

The properties required by the model are determined from available data derived from the Cone and LIFT apparatuses. These properties are as follows:

1. Ignition Temperature, T_{ig}	from cone or LIFT
2. Thermal Inertia, kρc	"
3. Lateral Flame Spread Parameter, Φ	from LIFT
4. Minimum Temperature for Lateral Spread, $T_{s,min}$	"
5. Heat of Combustion, ΔH_c	from cone
6. Effective Heat of Gasification, L	"
7. Total Energy per Unit Area, Q"	"

Three sets of materials will be discussed. The first set consists of 13 materials originally tested in Sweden in the room-corner test. These materials (S-series) are listed in Table 1. The properties were assembled by Cleary and Quintiere[5] from cone and LIFT data available from several sources. These materials are between 10 and 43 mm thick. A more complete description of the materials, and the results in the room-corner tests, are given by Sundström[2].

The second set of materials come from the EUREFIC program. These materials (E-series) and their derived properties are given in Table 2. These materials are between 12 and 80 mm thick. The cone data were taken from Thureson[6], and the LIFT data were taken from Nisted[7]. In the latter case, the raw data were reprocessed since there appeared to be some discrepancies in that report. Also ignition data from the cone were examined together with LIFT data in an attempt to derive more accurate values for T_{ig} and kρc. In some cases, this did not appear to improve accuracy since greater variations resulted. Hence, we used our values that were more consistent with values used by Karlsson[4] for these two properties.

The third set of materials represent aircraft cabin lining materials studied by the FAA several years ago in their program to improve the survivability in post-crash fires. The property data were obtained by Harkleroad[8] and Quintiere *et al.*[9] These properties are given for the F-series materials in Table 3.

In the current model an important input property is $\Delta H_c/L$. This is derived from the slope of the peak energy release rate per unit area versus the irradiance level in

Table 1. Flame Spread and Heat Release Properties of Swedish Fire Test Materials

Material	T_{ig} (°C)	kρc $(kW/m^2K)^2s$	Φ (kW^2/m^3)	$T_{s,min}$ (°C)	ΔH_c (kJ/g)	L (kJ/g)	Q" (MJ/m^2)
S1 Insulating Fiberboard	381	0.229	14	90	14	4.2	≥68.
S2 Medium Density Fiberboard	361	0.732	11	80	14	4.2	≥100
S3 Particle Board	405	0.626	8	180	14	5.4	≥120.
S4 Gypsum Board	469	0.515	14	380	7	4.8	2.8
S5 PVC Covered Gypsum Board	410	0.208	25	300	13	3.7	4.6
S6 Paper Covered Gypsum Board	388	0.593	0.5	300	10	4.8	7.2
S7 Textile Covered Gypsum Board	406	0.570	9	270	13	1.5	8.3
S8 Textile Covered Mineral Wool	391	0.183	6	174	25	2.8	9.3
S9 Melamine Covered Particle Board	483	0.804	<1	435	11	4.8	≥60.
S10 Expanded Polystyrene (PS)	482	0.464	31	130	28	1.5	32.
S11 Polyurethane Foam (rigid)	393	0.031	3	105	13	3.1	14.
S12 Wood Panel (Spruce)	389	0.569	24	155	15	6.3	≥120.
S13 Paper Covered Particle Board	426	0.680	13	250	13	6.5	≥100.

Table 2. Flame Spread and Heat Release Properties of the EUREFIC Materials

Material	T_{ig} (°C)	kρc $(kW/m^2K)^2s$	Φ (kW^2/m^3)	$T_{s,min}$ (°C)	ΔH_c (kJ/g)	L (kJ/g)	Q" (MJ/m^2)
E1 Painted GypsumPaper Plaster Board	551	0.73	3.3	478	4.1	3.6	3.3
E2 Ordinary Birch Plywood	392	0.99	13	164	11.9	6.2	75.5
E3 Textile Covering on Gypsum Board	387	0.97	7.7	189	7.5	3.1	9.5
E4 Melamine faced High Density Non-Combustible Board	631	0.32	12.7	527	8.5	3.5	7.0
E5 Plastic faced Steel Sheet on Mineral Wool	582	0.60	44	472	11.0	34.	2.5
E6 FR Particle Board Type B1	482	0.29	--	482	3.9	1.4	5.5
E7 Combustible faced Mineral Wool	354	0.11	0.86	263	11.0	9.2	1.7
E8 FR ParticleBoard	678	1.8	--	678	6.0	4.0	6.0
E9 Plastic faced Steel Sheet on Polyurethane Foam	494	0.60	22	326	12.0	5.1	17.0
E10 PVC Wallcarpet on Gypsum Board	391	0.69	8.2	367	6.5	3.3	11.0
E11 Extruded Polystyrene Foam	482	0.44	11.5	354	27.0	2.7	20.0

Table 3. Flame Spread and Heat Release Properties for the FAA Materials

Material	T_{ig} (°C)	kρc $(kW/m^2K)^2s$	Φ (kW^2/m^3)	$T_{s,min}$ (°C)	ΔH_c (kJ/g)	L (kJ/g)	Q" (MJ/m^2)
F1 Epoxy Fiberglass faced Nomex 1/4 in. Honeycomb Core	438	0.174	1.17	425	11.3	4.9	10
F2 Phenolic Fiberglass faced Nomex 1/4 in. Honeycomb Core	570	0.107	6.23	490	23	12.1	8.0
F3 Epoxy Kevlar faced Nomex 1/4 in. Honeycomb Core	465	0.188	4.86	400	11.4	5.7	9.0
F4 Phenolic Kevlar faced Nomex 1/4 in. Honeycomb Core	558	0.133	2.47	510	18.6	4.8	9.0
F5 Phenolic Graphite faced Nomex 1/4 in. Honeycomb Core	570	0.186	4.58	510	24.	68.8	7.0
ABS with 20% PVC 1/16 in. Sheet	388	0.76	6.63	282	15*	3.4+	27.0
Polycarbonate 1/16 in. Sheet	518	0.84	--	518	15*	1.6+	24.0
ULTEM 1/16 in. Sheet	585	0.91	--	585	15*	4.8+	11.0

---

* Estimated value

\+ Computed from estimated value of ΔH_c

the cone calorimeter. This will only yield appropriate results if the flame heat flux in the cone does not vary with irradiance. Since ΔH_c is derived from the cone data separately and is usually fairly constant, the uncertainty then arises in deriving L. Hence although the current model attempts to evaluate the energy release rate at the heat flux in the room-corner test, the uncertainty in this ratio can lead to problems. In the third set of materials, ΔH_c was not directly recorded for materials F6-8, but $\Delta H_c/L$ could be evaluated which allowed the model to be run without any deficiency of input data.

Room-Corner Test Scenario

A sketch of the room-corner test based on NT FIRE 025 is shown in Figure 3.

The corner floor burner is maintained at 100 kW for 10 minutes and then increased to 300 kW. In the model, this corresponds to a corner flame length of 1.3 m, followed by a flame which extends 1.2 m from the corner and along the ceiling (or an effective flame length of 3.6 m). The test is run to determine if and when the total energy release rate reaches 1 MW. The room-corner test results are available from Sundström[2] for the S-series, and from Söderbom[10] and Karlsson[4] for the E-series. Also computer files are available from Lønvik and Opstad[11]. However, we were not always able to identify the correct channel. Also the times to reach 1 MW appear to differ by 20s at most between those of Söderbom[10] and Karlsson[4].

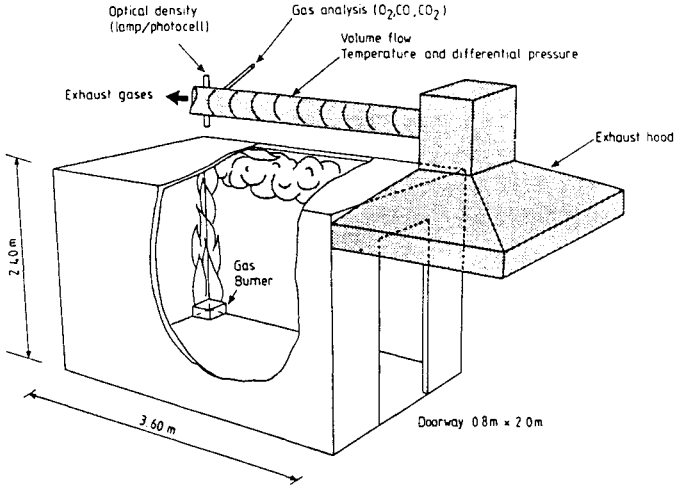

Figure 3. Room-Corner Test Configuration from Sundstrom[2].

We used the latter. The FAA F-series materials will be run by the model, and no experimental results exist to check the calculations. However, full-scale experiments were run for four of the materials (F1, F2, F4, and F5) in a post-crash wide-body aircraft fire scenario[12]. Hence, relative comparisons on rankings can be made for the FAA materials.

RESULTS

The times to reach 1 MW were compared to the experimental results for the S and E-series. In some cases, variations in the input property data were examined to see its effect on the time calculated. The time to reach 1 MW in hypothetical room-corner fire tests for the FAA materials is also reported. In all of the cases, lateral flame spread was insignificant because the minimum surface temperature for spread was not reached until at least 1 MW was reached. This characteristic was not reported on in the experiments, so the appropriateness of the model calculations can not be addressed in this regard. Also radiation feedback from the room only becomes a significant factor as the energy release rate approaches 1 MW. From the experimental results reported by Karlsson[4] at 1 MW the room gas temperature corresponds to approximately 500°C. This corresponds to a maximum possible radiant heat flux of 20 kW/m^2.

S and E-Series

Results for the S and E-series are reported in Table 4. The principal differences between the experimental and calculated times occur for cases that reach 1 MW after 10 minutes. Also this predominately occurs for thin materials on a noncombustible substrate. For example, S4 is unpainted gypsum wall board and E1 is painted gypsum wall board. The primary differences in these two materials is their $\Delta H_c/L$. values,

Table 4. Time(s) to Reach 1 MW

	Exp.	Calc.	Variation	Comment on Variation
S1	59	29	36	1.25L
S2	131	91	120	1.25L
S3	157	121	167	1.25L
S4	∞	642	∞	1.25L & 0.5Q"
S5	611	30	602	1.25L & 0.5Q"
S6	640	613		
S7	639	41	606	1.25L & 0.5Q"
S8	43	12		
S10	115	44		
S11	6	4		
S12	131	110	156	1.25L
S13	143	222	148	0.75L
E1	∞	∞		
E2	160	265		
E3	670	∞	608	1.2(300 kW flame length)
E4	∞	646		
E5	∞	∞		
E6	630	∞		
E7	75	601		
E8	∞	∞		
E9	215	504	71	0.28kρc
E10	650	614		
E11	80	47		

i.e., 1.5 for S4 and 1.1 for E1. By increasing L by 25% and reducing Q" by 50% for S4 gives calculated results that are in agreement with the experiment. For the thin materials, the burn-out front can be initiated; and if it catches up to the pyrolysis front, the fire will die out. This is illustrated in Figures 4A and 4B for E1 where the energy release rates are compared, and the computed upward pyrolysis and burn-out fronts are shown as a function of time. The energy release rate of the painted gypsum board reaches a maximum of approximately 300 kW while the experimental results are about 100 kW over the 300 kW burner contribution. The pyrolysis front is initiated as E1 ignites due to the 100 kW burner fire at about 90 sec. The burn-out front commences at about 180 sec as the painted paper burns away in the ignition region. Shortly after, the fronts coincide. But when the burner energy release rate is increased to 300 kW at 600 sec, the pyrolysis front accelerates initially faster than the burn-out front due to the flame extension caused by the burner. Once the pyrolysis front gets beyond the region of influence of the burner flame, the fire again dies out. This is governed by the length of the burner flames and by the dimensionless quantity,

$$b = k_f \dot{Q}'' - 1 - t_{ig} / t_b \qquad (14)$$

according to Cleary and Quintiere[5]. If b > 0 acceleration is possible, and if b < 0 the fire can die out. In the calculations, b varies with time so it is not obvious how to deduce a criterion for this behavior from the properties alone.

In Table 4, it should be noted that comparable variations in L for thick combustible materials (25 percent) do not cause the same degree of differences in the times to reach 1 MW as for the thin materials. Also for material E3, better agreement of the calculated result with the experiment was achieved by increasing the burner flame length at 300 kW by 20 percent. This flame

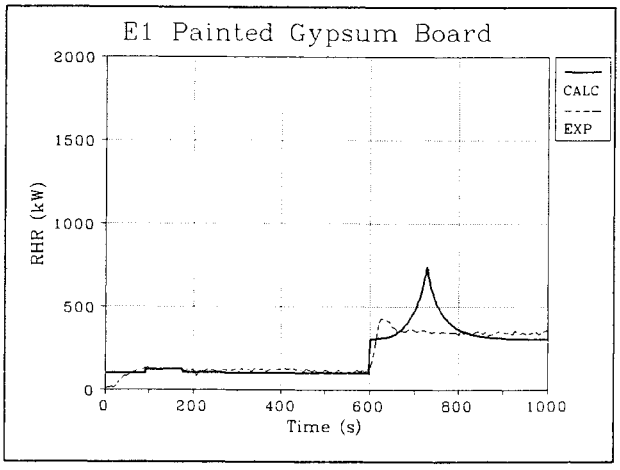

Figure 4A. A Comparison of the Energy Release Rate (RHR) for Material E1: Experiment and Calculation.

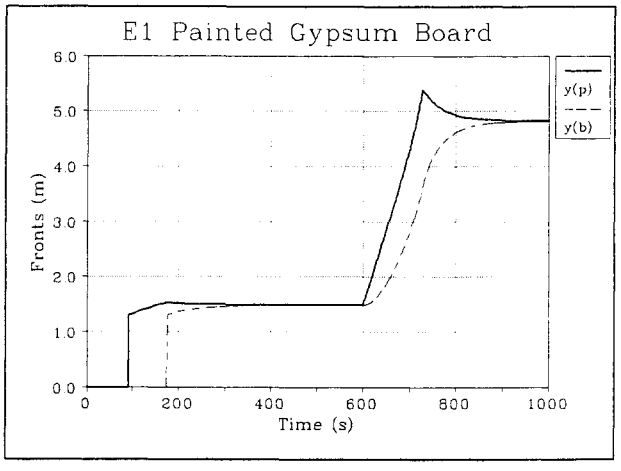

Figure 4B. The Calculated Upward Pyrolysis and Burn-out Fronts for Material E1.

length is more consistent with the correlation given by Karlsson[4]. For material E9, a wide variation in kρc occurred, and reducing the selected value by nearly 75 percent gave calculated results that bracketed the experimental time. In all of the variations considered, the variation was within the bounds of the uncertainty for the deduced properties. It is not clear whether more careful and complete data can reduce this uncertainty, or whether the materials

themselves may have significant property variations due to their construction. In some cases, the method of bonding the components of the composite materials could be a factor. Furthermore, it is recognized that this analysis of the parameter variations is not systematic nor complete. It is only offered to display the sensitivity of the results to these variations.

Since it may be difficult to assess the overall accuracy of the calculated results listed in Table 4, a graph is plotted in Figure 5. In 8 of the 24 cases, poor agreement is seen. However, in 5 of these 8 cases, relatively small changes in the input properties brought the calculations into more consistent agreement with the experimental results. Four of these five materials were thin combustibles on an inert substrate.

Other results are shown for illustration in Figures 6 and 7 for materials E2, plywood, and E3, textile wall covering on gypsum board.

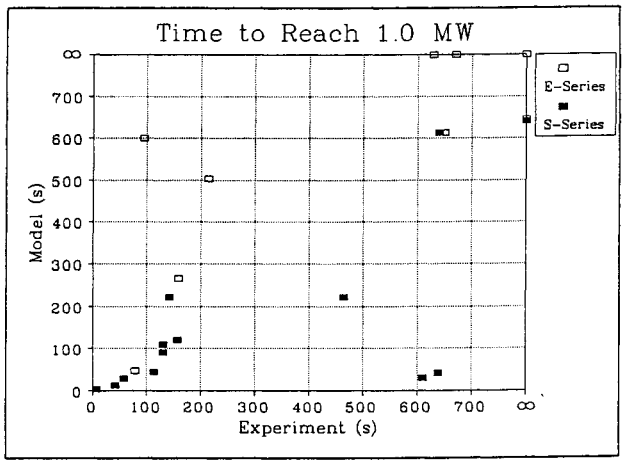

Figure 5. Model Calculated Times to Reach 1 MW Compared to the Experimental Results for the S and E-Series.

FAA Materials, F-Series

Figure 8 shows the simulated room-corner results for the aircraft materials. The materials F1, epoxy fiberglass, and F4, phenolic kevlar, are the worst; and F5, phenolic graphite, is the best. Table 5 lists the times to reach 1 MW along with the times for the materials to ignite due to the 60 kW/m^2 burner heat flux. Also listed in Table 5 are the approximate times to flashover found in the post-crash fire experiments conducted by Hill, Eklund and Sarkos[12] which contained seats as well as the lining materials considered. Only four of the materials were tested with seats. The results are somewhat consistent except that the tests

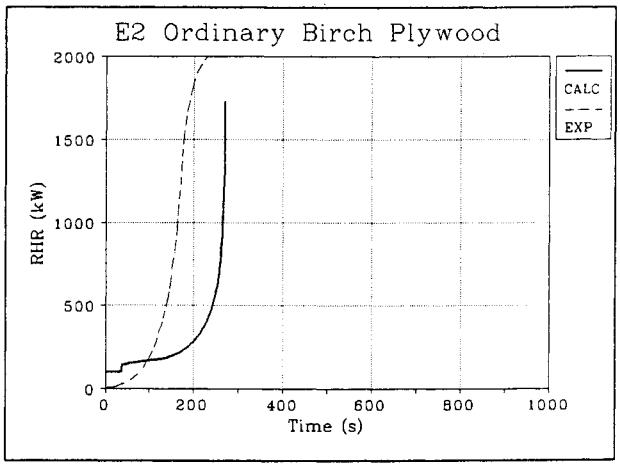

Figure 6. A Comparison of the Energy Release Rate (RHR) for Material E2: Experiment and Calculation.

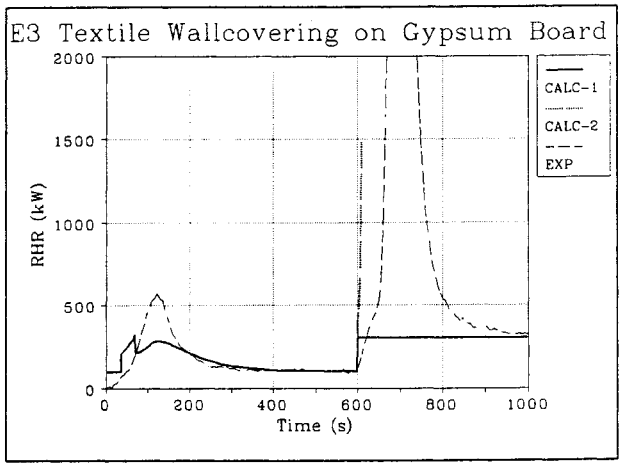

Figure 7. A Comparison of the Energy Release Rate (RHR) for Material E3: Experiment and Calculation.

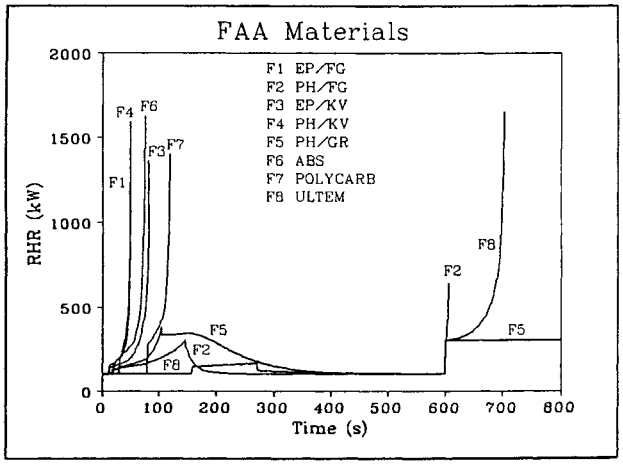

Figure 8. Calculated Rate of Energy Release (RHR) for the Aircraft Materials in the Room-Corner Test.

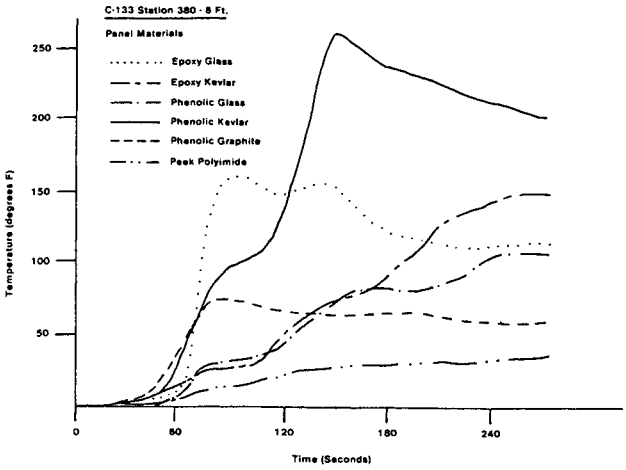

Figure 9. C-133 Cabin Gas Temperature for the Panel Tests Without Seats from Hill, Eklund And Sarkos[12].

Table 5. Calculated Room-corner Test Results for Aircraft Materials, F-Series, and Comparison to the Post-Crash C-133 Tests by Hill[12]

	Room-Corner Test Results		C-133 Post-Crash Fire Tests
	Ignition Time (s)	Time to 1 MW (s)	Flashover Time with Seats (s)
F1 Epoxy Fiberglass faced Nomex 1/4 in. Honeycomb Core	10	50	70
F2 Phenolic Fiberglass faced Nomex 1/4 in. Honeycomb Core	16	606	230
F3 Epoxy Kevlar faced Nomex 1/4 in. Honeycomb Core	12	81	--
F4 Phenolic Kevlar faced Nomex 1/4 in. Honeycomb Core	18	49	70
F5 Phenolic Graphite faced Nomex 1/4 in. Honeycomb Core	28	∞	190
F6 ABS with 20 % PVC 1/16 in. Sheet	29	73	--
F7 Polycarbonate 1/16 in. Sheet	80	119	--
F8 ULTEM 1/16 in. Sheet	158	699	--

reverse the order of F2 and F5, making the phenolic fiberglass panel better than the phenolic graphite panel.

Figure 9 shows the cabin temperature response to the post-crash fire experiments for the case of the cabin tests with the panels only. Flashover conditions were not produced in these tests due to the lack of influence of the seats. Also ignition of the panel materials would depend on the interaction of the external fuel fire, which could be spurious. If one interprets the area under the temperature curves as a

measure of the performance of the panel materials, then this order of performance (F4, F1, F3, F2, F5, worst to best) is consistent with the calculated times to reach 1 MW in the room-corner test simulations.

Conclusions

The model appears to predict consistent results with the experiments for the time to reach 1 MW in 2 out of every 3 of the 24 E and S tests. It was found that some reasonable changes in either the input properties or the phenomenological specifications can improve the agreement. It is not clear whether the uncertainty in the property data could be reduced by more careful and complete experiments using the cone and the LIFT apparatuses. Critical areas needed for examination in the model include the computation of the energy release rate per unit area, the heat fluxes, and the flame lengths specified for the burner flame. The extension of the upward spread equations to the ceiling and ceiling jet regions can only be regarded as a crude estimate, but must suffice until results for these phenomena are forthcoming from research.

The application of the model to the aircraft materials could be viewed as reasonably successful in terms of the apparent consistency with the limited results of the post-crash fire tests. It should be noted that the current model is not limited to the simulation of the room-corner test scenario, and could be modified with its current scope to address aspects of aircraft cabin fires or other room fire configurations.

Acknowledgement

This work was prepared for the International Conference for the Promotion of Advanced Fire Resistant Aircraft Interior Materials, February 9-11, 1993, FAA Technical Center, Atlantic City, NJ. It was supported, in part, by the SFPE Student Research Grant Program.

Nomenclature

A	area
b	parameter defined in Equation 14
c	specific heat
d	depth of room
D	side of square burner
g	acceleration due to gravity
h	convective heat transfer coefficient
H	height of room, vent
k	thermal conductivity
k_f	empirical constant, Equation 7
L	effective heat of gasification
n	empirical power, Equation 7
q	heat
Q	energy release
t	time
T	temperature
w	width of room
x	lateral position
y	upward position
z	downward position
ρ	density
τ	dummy variable for time, Equation 1
ΔH	heat of combustion

Subscripts

b	burn-out
f	flame
ig	ignitor, ignition
min	minimum
p	pyrolysis
s	surface
s,o	surface responding to ignitor flame heat flux
o	initial
∞	ambient

Superscripts

$\dot{(\ )}$	per unit time
$(\ )'$	per unit width
$(\ )''$	per unit area

REFERENCES

1. Quintiere, J. G., "A Simulation Model for Fire Growth on Materials Subject to a Room-Corner Test," *Fire Safety Journal*, Vol. **18**, 1992.

2. Sundström, B., "Full-Scale Fire Testing of Surface Materials," Technical Report SP- RAPP 1986:45, Swedish National Testing and Research Institute, Boras, Sweden, 1986.

3. Wickström, U. and Göransson, U., "Full-scale/Bench-scale Correlations of Wall and Ceiling Linings," *Fire and Materials*, Vol. **16**, 1992, pp. 15-22.

4. Karlsson, B., "Modeling Fire Growth on Combustible Lining Materials in Enclosures," 992, Report TVBB-1009, Lund University, Department of Fire Safety Engineering, Lund, Sweden, 1992.

5. Cleary, T. G. and Quintiere, J. G., "A Framework for Utilizing Fire Property Tests," *Fire Safety Science - Proc. of the 3rd International Symposium*, ed. G. Cox and B. Langford, Elsevier Applied Science, London, 1991.

6. Thureson, P., "EUREFIC-Cone Calorimeter Test Results," SP Report 1991:24, SP Swedish National Testing and Research Institute, Boras, Sweden, 1991.

7. Nisted, T., "Flame Spread Experiments in Bench Scale," Dantest, Fire Technology, København, Denmark, 1991.

8. Harkleroad, M., "Ignition and Flame Spread Measurements of Aircraft Lining Materials," NBSIR 88-3773, National Bureau of Standards (NIST), Gaithersburg, MD, 1988.

9. Quintiere, J. G., Babrauskas, V., Cooper, L., Harkleroad, M., and Steckler, K., "The Role of Aircraft Panel Materials in Cabin Fires and their Properties," DOT/FAA/CT-84/30, Federal Aviation Administration, Technical Center, Atlantic City Airport, NJ, 1985.

10. Söderbom, J., "EUREFIC-Large Scale Tests according to ISO DIS 9705," SP Report 1991:27, SP Swedish National Testing and Research Institute, Boras, Sweden, 1991.

11. Lønvik, L. E., and Opstad, K., "Software User's Guide for DCS, A Data Converting System," Report No. STF25 A90003, SINTEF, Trondheim, Norway, 1991.

12. Hill, R. G., Eklund, T. I., and Sarkos, C. P., "Aircraft Interior Panel Test Criteria Derived from Full-Scale Fire Tests," DOT/FAA/CT-85/23, Federal Aviation Administration, Technical Center, Atlantic City Airport, NJ, 1985.